

## Gate-tunable and High Optoelectronic Performance in Multilayer WSe<sub>2</sub> P-N Diode

Received 00th January 20xx,  
Accepted 00th January 20xx

Yujue Yang, †<sup>a</sup> Nengjie Huo †<sup>a</sup> and Jingbo Li \*<sup>a,b</sup>

DOI: 10.1039/x0xx00000x

www.rsc.org/

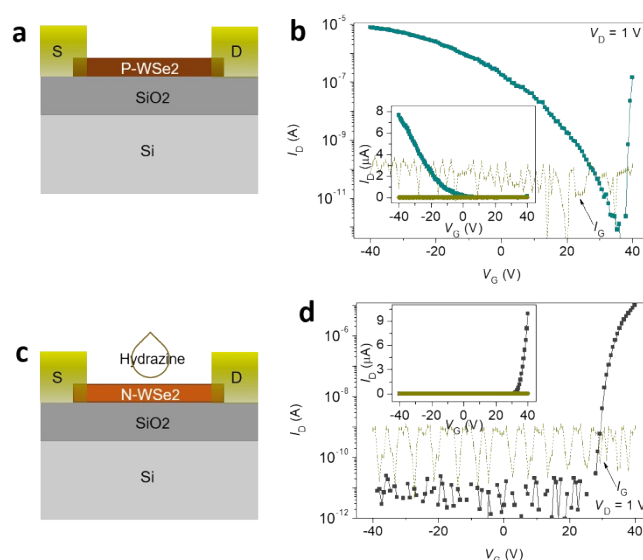


**Fig. S1** (a) Schematic diagram of pristine WSe<sub>2</sub> transistor. (b) Transfer curves of the device showing the main P-type behaviour with ON-OFF ratio up to 10<sup>7</sup>. Insert is the same curve with linear scale. (c) Schematic diagram of WSe<sub>2</sub> transistor after chemically doping. (d) Transfer curves of the device showing the well N-type behaviour with ON-OFF ratio over 10<sup>6</sup>. Insert is the same curve with linear scale. The yellow curves in (b) and (d) represent the leakage current ( $I_G-V_G$ ), which is negligible compared to the source-drain current, ensuring the measured current signal is from the WSe<sub>2</sub> channel.

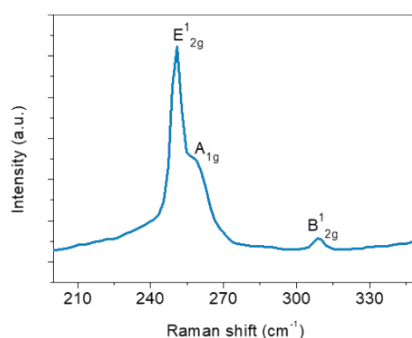


**Fig. S2** Raman spectra of the WSe<sub>2</sub>, showing the typical phonon mode of multilayer WSe<sub>2</sub>. The two adjacent modes at around 250 nm are assigned to E<sup>1</sup><sub>2g</sub> and A<sub>1g</sub> modes, respectively. The normally inactive mode B<sup>1</sup><sub>2g</sub> mode can emerge at multilayer WSe<sub>2</sub> but disappear at monolayer. Our Raman result is consistent with previous reports.<sup>[S1,S2]</sup>

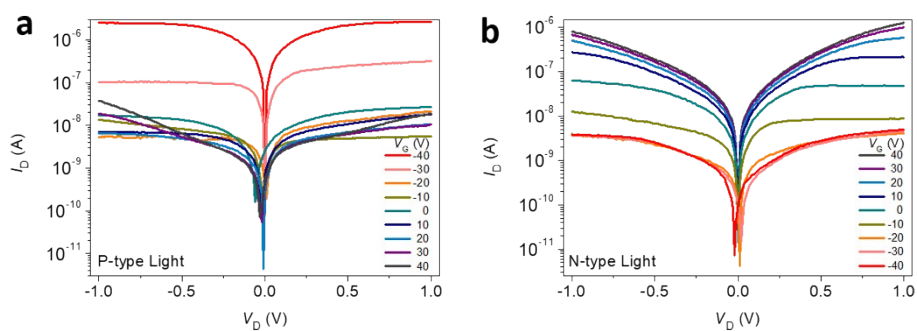


**Fig. S3** (a) Output curves of pristine P-type WSe<sub>2</sub> transistors under light illumination. (b) Output curves of the doped N-type WSe<sub>2</sub> transistors under light illumination. The photovoltaic effect is absent in both case.

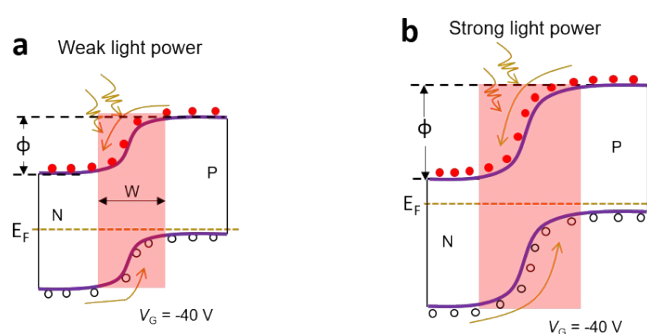


**Fig. S4** Schematic diagram of band structures in the P-N junctions at  $V_G$  of -40 V under (a) weak and (b) strong light illumination. The red shadow region represents the depletion region of the P-N junctions.

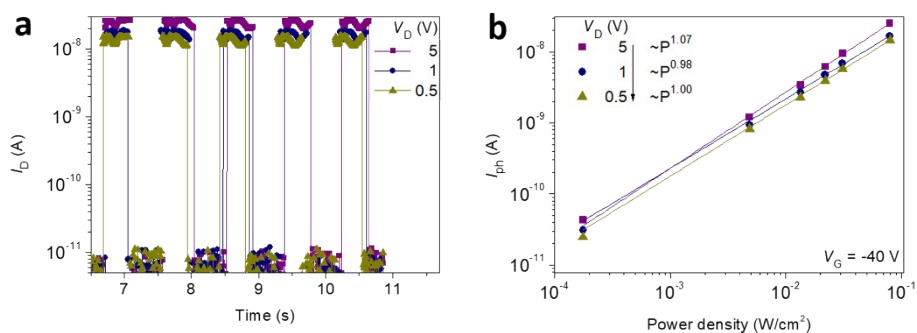


**Fig. S5** (a) Temporal response the WSe<sub>2</sub> photodiode at different  $V_D$ , showing the fast speed below 4 ms and light switching ratio over  $10^3$ . (b) Photocurrent of the device as a function of incident light power density at  $V_G$  of -40 V and different  $V_D$ . The linear curves are the power-law fits, describing fitted  $\alpha$  of  $\sim 1$ .

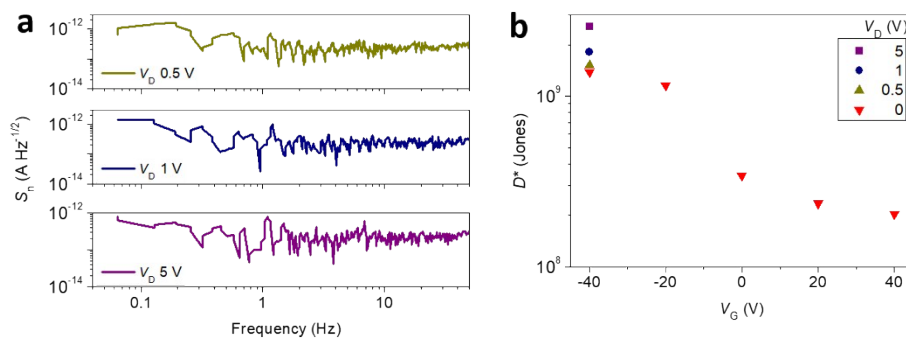


**Fig. S6** (a) Noise spectral density  $S_n$  of the photodiode at different  $V_D$ . To obtain  $S_n$ , the dark current traces were measured with the Agilent system (Agilent B1500A) under exactly the same conditions as the optical measurements were performed (same  $V_G$  and  $V_D$ ) at a sampling rate of 250 Hz. We obtained noise spectral density by calculating the Fourier transformation of dark current traces. (b) The calculated specific detectivity  $D^*$  at different  $V_D$  and  $V_G$ , showing the maximum  $D^*$  of  $2.5 \times 10^9$  Jones at  $V_D$  of 5 V and  $V_G$  of -40 V.

### Supplementary References

1. H. Li, G. Lu, Y. Wang, Z. Yin, C. Cong, Q. He, L. Wang, F. Ding, T. Yu and H. Zhan, *Small*, 2013, **9**, 1974.
2. N. Huo, S. Tongay, W. Guo, R. Li, C. Fan, F. Lu, J. Yang, B. Li, Y. Li and Z. Wei, *Adv. Electron. Mater.*, 2015, **1**, 1400066.